

Supporting Information

In Situ Constructed Topological Rich-Vacancy-Defects Nitrogen-doped Nanocarbons as High-Effective Metal-Free Oxygen Catalysts for Li-O₂ Batteries

Zemin Sun,^{[a],#} Liu Lin,^{[a],#} Yaqing Wei,^[a] Mengwei Yuan,^[a] Huifeng Li,^[a] Caiyun Nan,^[a] Kuibo Yin,^[b] Genban Sun,^{[a],*} Run Long,^{[a],*} Xiaojing Yang^{[a],*}

^aBeijing Key Laboratory of Energy Conversion and Storage Materials and College of Chemistry, Beijing Normal University, Beijing 100875, China

^bSEU-FEI Nano-Pico Center, Key Lab of MEMS of Ministry of Education, Southeast University, Nanjing 210096, PR China

Zemin Sun and Liu Lin are equally contribution.

Corresponding Author

*E-mail: gbsun@bnu.edu.cn (G. Sun); runlong@bnu.edu.cn (R. Long); yang.xiaojing@bnu.edu.cn (X. Yang)

Experimental Section

Synthesis of g-C₃N₄: The white melamine was heated at 550 °C for 6 hour in a corundum rectangular ship with a cover under Ar flowing. The product was yellow powder as shown in Figure S1b.

Synthesis of TRNC: 5g as-prepared g-C₃N₄ was mixed with 5g magnesium powder and then heated at 750 °C for 2 hour under Ar flowing in a corundum rectangular ship with a cover. The product was dark powder and washed by enough dilute CH₃COOH to remove the excess Mg and its compounds, and then it was washed through distilled water with repeated centrifugation (10000 rpm, 5 min). Finally, the product was dried at 40 °C in vacuum overnight and signed as topological rich-vacancy-defects nitrogen-doped nanocarbon (TRNC) as shown in Figure S1c.

Materials Characterization

The crystal phase of products were characterized by X-ray diffraction (XRD) on a Phillips X'pert ProMPD diffractometer (Cu K α , $\lambda = 1.54056 \text{ \AA}$). The generator setting was 40 kV and 40 mA within 5-90°. SEM images were characterized by a field emission scanning electron microscopy (FESEM, S-8010, Hitachi) at an acceleration voltage of 10 kV. TEM images and selected area electron diffraction (SAED) patterns were performed by a high-resolution transmission electron microscope (HRTEM, JEM-2010, JEOL and FEI Technai G2 F20) at an acceleration voltage of 200 kV. The X-ray photoelectron spectroscopy (XPS) was recorded on ESCALAB 250Xi spectrometer (Thermo Fisher) with Al K α radiation as the X-ray source for excitation to characterize the surface composition of the samples. Raman spectra were collected from 800 to 2000 cm⁻¹ on a microscopicconfocal Raman spectrometer (LabRAMAramis, Horiba JobinYivon) using a 532nm He-Ne laser. The specific surface areas were characterized by the Brunauer-Emmett-Teller (BET) method. The pore size distribution was derived from the desorption branch using the Barrett-Joyner-Halenda (BJH) method.

Electrochemical measurement

The Li-O₂ battery measurements were conducted in CR2032 coin cells. All the cells were assembled in a glove box filled with argon, consisting of a Li foil anode, a glass fiber filter separator, an air electrode and electrolyte (1 M LiTFSI in TEGDME). To prepared the air electrodes, g-C₃N₄,

TRNC or Ketjenblack (KB) (45 wt%), KB (45 wt%) and poly-vinylidene fluoride (PVDF) binder (10 wt%) were mixed and added NMP to form a homogenous slurry. Then the slurry was coated on the carbon papers and dried at 80 °C in vacuum for 12 h to form the air electrodes. The current density and specific capacity were calculated according to the amount of KB. The electrochemical impedance spectrums of the cells were evaluated by AC impedance over the frequency range from 0.01 to 10⁵ Hz with an amplitude of 5 mV. Linear sweep voltammetry (LSV) and cyclic voltammetry (CV) were also measured on an electrochemical workstation (Zennium IM6 station).

Computational Methods

The calculations were performed using the Vienna ab initio simulation package (VASP).^[1] The electron exchange and correlation energy was treated with the generalized gradient approximation of the Perdew-Burke-Ernzerhof (PBE).^[2] The core and electrons interactions were described by the projected augmented wave (PAW) approach.^[3] The energy cutoff of plane wave basis was set to 400 eV. The van der Waals (vdW) interactions was described using the DFT-D3 method of Grimme.^[4] A Γ -centered 4 × 4 × 1 Monkhorst-Pack k-point mesh was used for all calculations. A 4 × 4 *P6₃/mmc* graphene supercell containing 32 atoms, separated by a vacuum region of 15 Å along the plan normal direction, was adopted in this work. The optimization stopped until energy difference between two ion steps is less than 1×10⁻⁵ eV.

The Gibbs free energy (G) is obtained based on the following equation:^[5]

$$G = E + E_{ZPE} - TS - neU$$

where E , E_{ZPE} , S , n and U are the DFT total energy, zero point energy, entropy, the number of electrons involving in reaction and electrode potential, respectively. For the overpotentials (η) of ORR and OER reactions, they are calculated as $\eta_{\text{ORR}} = U_0 - U_{\text{DC}}$ and $\eta_{\text{OER}} = U_{\text{C}} - U_0$. Here, U_0 , U_{DC} and U_{C} represent the equilibrium potential, maximum potential for discharging and minimum potential for charging, respectively.

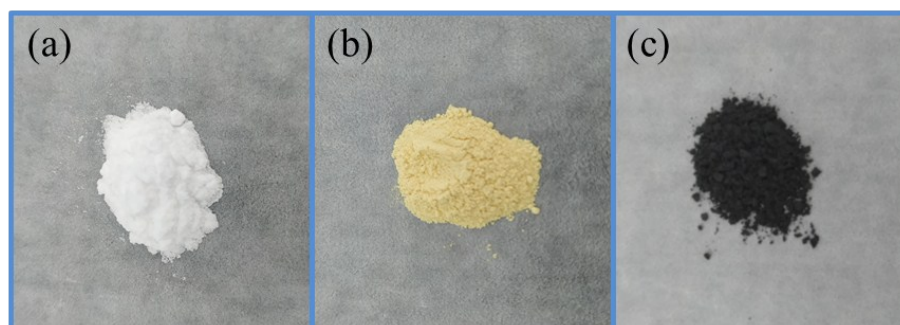


Figure S1 Photographs of (a) melamine, (b) g-C₃N₄ and (c) TRNC.

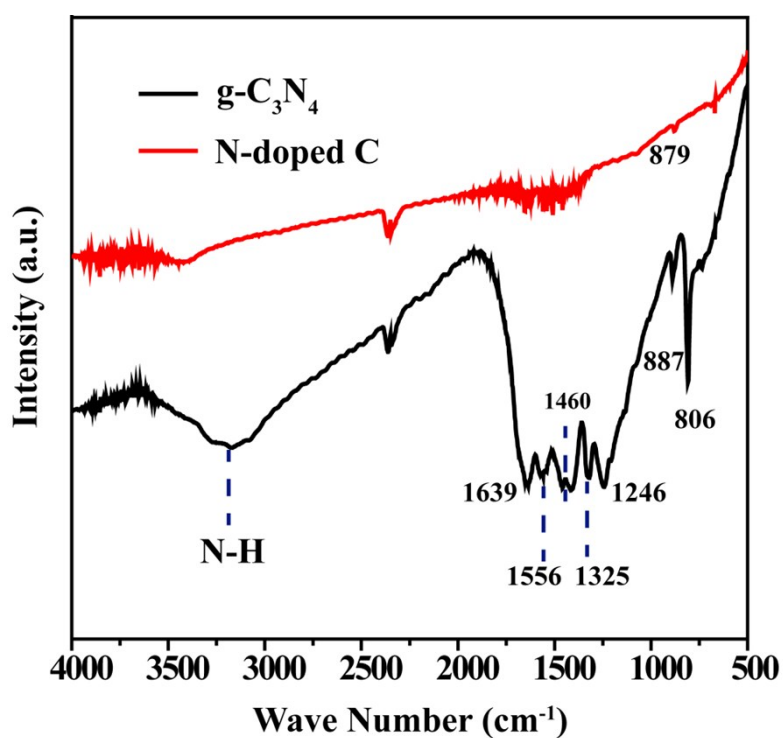


Figure S2 FT-IR spectra of g-C₃N₄ and TRNC.

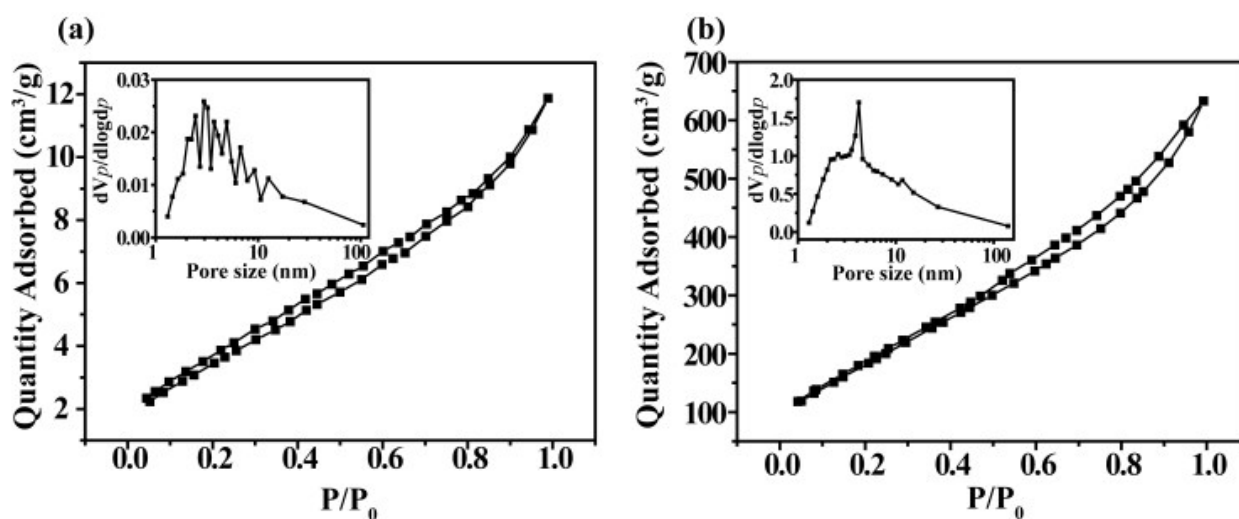


Figure S3 Nitrogen adsorption/desorption isotherms of (a) g-C₃N₄ and (b) TRNC. The insets show the corresponding pore size distributions.

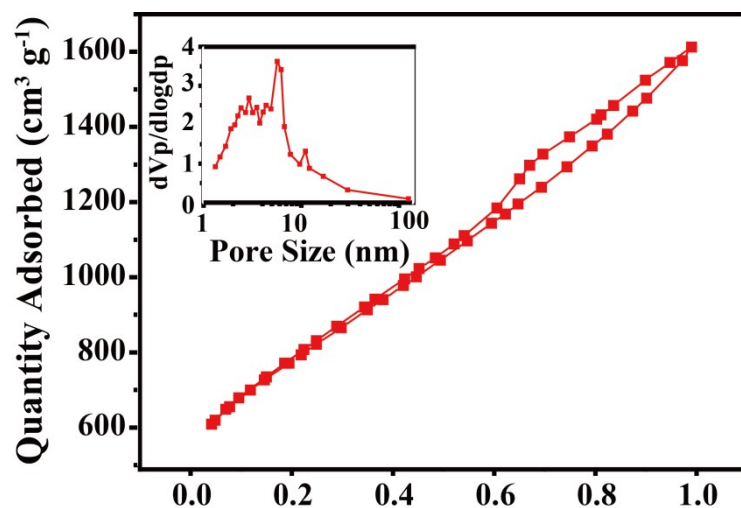


Figure S4 Nitrogen adsorption/desorption isotherms of KB. The insets show the corresponding pore size distributions.

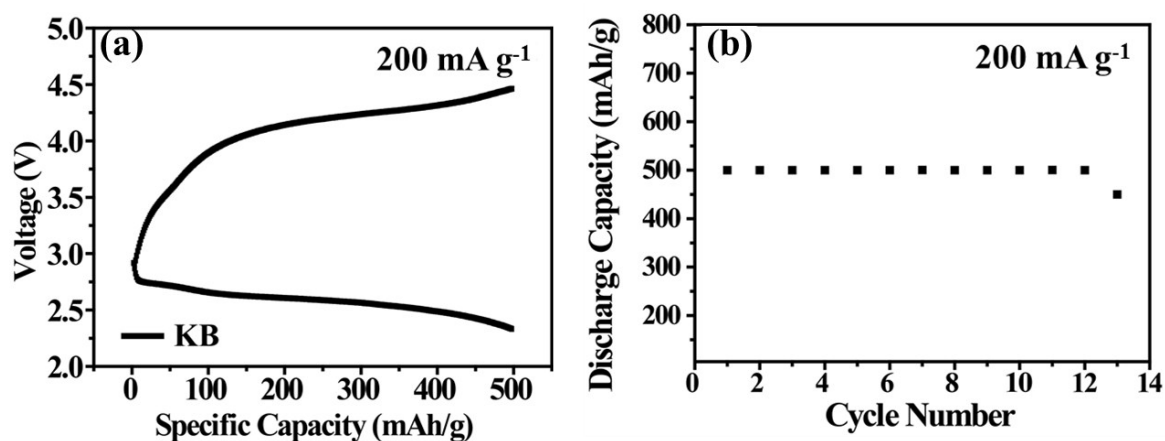


Figure S5 (a) The first cycle of KB with a capacity limitation of 500 mAh g⁻¹ at 200 mA g⁻¹. (b)

The cycle performance of KB at 200 mA g⁻¹.

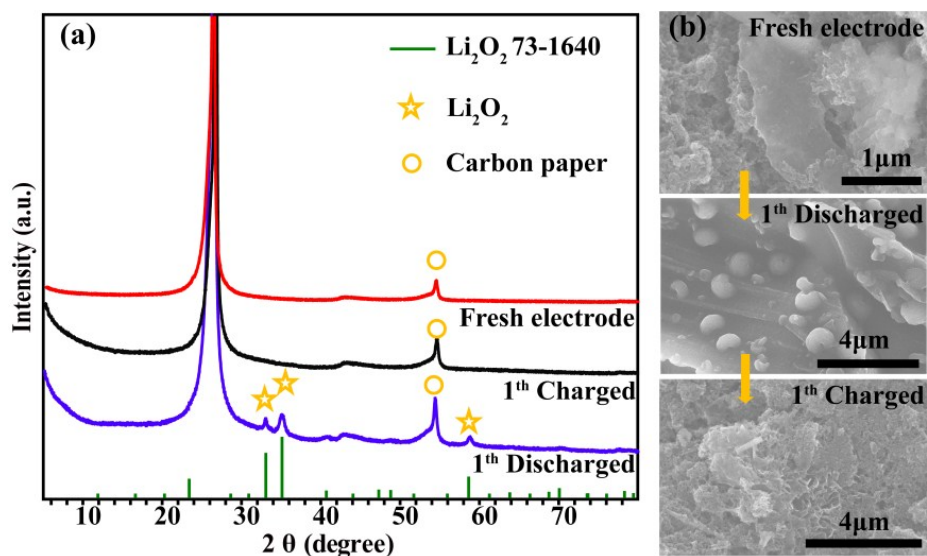


Figure S6 (a) XRD patterns and (b) FESEM images of TRNC in different states.

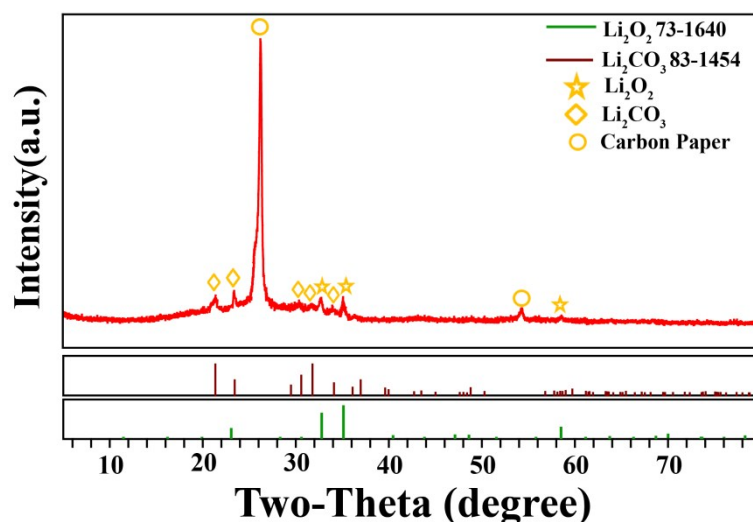


Figure S7 XRD patterns of discharged TRNC electrode after 200 cycles.

Table S1 Comparison of Li-O₂ batteries' performance of the present work with other catalysts

Catalysts	Specific Surface area	Limit capacity (mAh g ⁻¹)/current density	Cycles	Ref.
TRNC	927.7 m ² g ⁻¹	500/500 mA g _{carbon} ⁻¹	>270	This work
ordered mesoporous carbon	1459 m ² g ⁻¹	500/200 mA g _{carbon} ⁻¹	11	S6
macroporous-mesoporous carbon	1386 m ² g ⁻¹		55	
CNTs	611.1 m ² g ⁻¹	500/0.1 mA cm ⁻²	<10	S7
Hollow Graphene Nanocages	374 m ² g ⁻¹	1000/100 mA g _{carbon} ⁻¹	10	S8
AGCA	2244 m ² g ⁻¹	1500/300 mA g _{carbon} ⁻¹	<30	S9
mesoporous graphene-like carbon	505.9 m ² g ⁻¹	500/100 mA g _{carbon} ⁻¹	6	S10

CMK-3	912.5 m ² g ⁻¹	2000/500 mA g _{carbon} ⁻¹	30	S11
Co@N-CFs	301.52 m ² g ⁻¹	500/100 mA g _{carbon} ⁻¹	<45	S12
CNTs	165.52 m ² g ⁻¹		<5	
hierarchically porous carbon	378 m ² g ⁻¹	2000/0.5 mA cm ⁻²	<11	S9

Reference

- [S1] G. Kresse, J. Furthmüller, *Phys. Rev. B*, 1996, **54**, 11169-11186.
- [S2] J. P. Perdew, K. Burke, M. Ernzerhof, *Phys. Rev. Lett.* 1996, **7**, 73865-3868.
- [S3] P. E. Blöchl, *Phys. Rev. B*, 1994, **50**, 17953-17979.
- [S4] S. Grimme, J. Antony, S. Ehrlich, H. Krieg, *J. Chem. Phys.* 2010, **132**, 154104.
- [S5] X. Ye, W. A. Shelton, *J. Chem. Phys.* 2010, **133**, 4521.
- [S6] D. Y. Kim, X. Jin, C. H. Lee, D. W. Kim, J. Suk, J. K. Sho, J. M. Kim, Y. Kang, *Carbon*, 2018, **13**, 118-126.
- [S7] Q. Lin, Z. Cui, J. Sun, H. Huo, C. Chen, and X. Guo, *ACS Appl. Mater. Interfaces*, 2018, **10**, 18754–18760.
- [S8] F. Wu, Y. Xing, X. Zeng, Y. Yuan, X. Zhang, R. S. Yassar, J. Wen, D. J. Miller, L. Li, R. Chen, J. Lu, and K. Amine, *Adv. Funct. Mater.* 2016, **26**, 7626–7633
- [S9] C. H. J. Kim, C. V. Varanasi and J. Liu, *Nanoscale*, 2018, **10**, 3753–3758.
- [S10] X. Lin, Y. Cao, S. Cai, J. Fan, Y. Li, Q. Wu, M. heng and Q. Dong, *J. Mater. Chem. A*, 2016, **4**, 7788–7794.
- [S11] E. Yoo and H. Zhou, *ChemSusChem*, 2016, **9**, 1249 – 1254.
- [S12] Y. Cao, H. Lu, Q. Hong, J. Bai, J. Wang, X. Li, *J. Power Source.*, 2017, **368**, 78-87
- [S13] Z. Wang, D. Xu, J. Xu, L. Zhang, X. Zhang, *Adv. Funct. Mater.* 2012, **22**, 3699–3705